UV-Sensitive Low Dark-Count PureB Single-Photon Avalanche Diode

Lin Qi, K. R. C. Mok, Edoardo Charbon
and Lis. K. Nanver
Department of Microelectronics
Delft University of Technology
Delft, the Netherlands
L.Qi@tudelft.nl

Mahdi Aminian and Edoardo Charbon
Advanced Quantum Architecture Laboratory
Ecole Polytechnique Fédérale de Lausanne
Lausanne, Switzerland

***Abstract* — A single-photon avalanche diode (SPAD) with high responsivity in the ultraviolet (UV) wavelength range has been fabricated on Si using PureB (Pure Boron) chemical-vapor deposition to create both a nanometer-thin anode junction and robust light entrance window. The device shows high responsivity at the wavelength of 330 nm and 370 nm when operating in Geiger mode. The dark count rates (DCR) can be as low as 5 Hz at room temperature for an active area of 7 μm^2. An implicit guard ring, using an n-enhancement implantation in the central region of the diode, is applied instead of peripheral diffused p-type guard rings to achieve a high fill-factor.**

I. INTRODUCTION

With PureB technology, Si photodiode detectors have been fabricated and commercialized with outstanding performance for low penetration-depth beams such as vacuum/extreme UV (VUV/EUV) light and low-energy electrons [1]. The PureB layer is formed by a pure-boron chemical vapor deposition (CVD) in a manner that allows integration of bare 2-nm-thin boron layers as front-entrance windows [2]. At the same time the PureB layer provides an effective p^+-doping of the semiconductor surface to form a nm-thin p^+n junction. In addition, to achieve high responsivity and stability in the beyond-visual spectral ranges it is important that a 2-nm thin PureB layer can be integrated as a robust and almost non-absorbing front-entrance window. This layer is conductive, does not oxidize and does therefore not charge during irradiation. Moreover, it is chemically resistant in many situations, and it can be used to form a barrier against silicidation/spiking of metals like Al [3], which can be removed selectively to the PureB layer. Thus, the fabricated Si photodiodes have surpassed the performance of other existing technologies on points such as internal/external quantum efficiency, dark current, and responsivity degradation.

Up until now this technology has been used for large area photodiodes operating at low reverse bias voltages. The present work has been performed to extend the capabilities of PureB photodiodes, so that highly sensitive imaging arrays with micron-sized pixels can be fabricated. High-sensitivity and exceptional speed are achieved by creating single-photon avalanche diodes (SPADs), that in recent years have received renewed interest due to wide applicability and versatility [4]. In our case, a p-n junction is fabricated in PureB technology and operated as an avalanche photodiode in Geiger-mode by biasing it well above breakdown. To prevent edge breakdown, a guard ring is generally implemented around the active area, generally a circle of 5 to 50 μm in diameter. The requirement of small device dimensions complicates the processing with respect to the fabrication of the guard rings and the opening of the light entrance windows. The former has been solved by introducing an implicit guard ring, using an n-enhancement implantation in the central region of the diode instead of a peripherally diffused p-type guard ring, and the latter has demanded a careful selective removal of the anode metallization.

II. DEVICE FABRICATION

To achieve high-sensitivity despite the small size, a design for operation in Geiger-mode is realized. A schematic cross section of the process flow for fabricating PureB SPADs is shown in Fig. 1. Starting with p-type (100) 2-5 Ωcm Si substrates, a 1.0-μm-thick n^- epitaxial layer is grown on an n^+ buried layer, which is contacted by implanted n^+ plugs. An n-enrichment is implanted through a 30-nm thermal silicon oxide to define the active region of the detector followed by the deposition of a 300-nm LPCVD TEOS. The implants are annealed at 950 °C for 20 min in argon gas. The anode contact windows are plasma-etched to the Si with soft landing and native oxide is removed by dip etching in HF 0.55% and Marangoni drying. Then the PureB layer is deposited from diborane in an ASM Epsilon 2000 reactor for 6 min at 700 °C and driven in for 1 min at 850 °C to form the p^+ region, the resulting junction depth is around 12 nm as shown from the TCAD simulated doping profile in Fig. 2. Right after the PureB deposition, 675 nm pure Al is sputtered at 50 °C, directly onto the PureB layer. Then, the cathode contact windows are opened by plasma etching. Another 675-nm Al layer containing 1% Si layer is deposited, also at 50 °C. After

metal patterning, the light entrance windows are opened and aligned to the n-enrichment region, first by plasma etching until 100 – 200 nm Al is left and then by removing the remaining Al by wet etching in HF 0.55% for 3 to 5 min. At last, a 400 °C alloy step in forming gas is performed to improve the contact between the Al and the PureB layer.

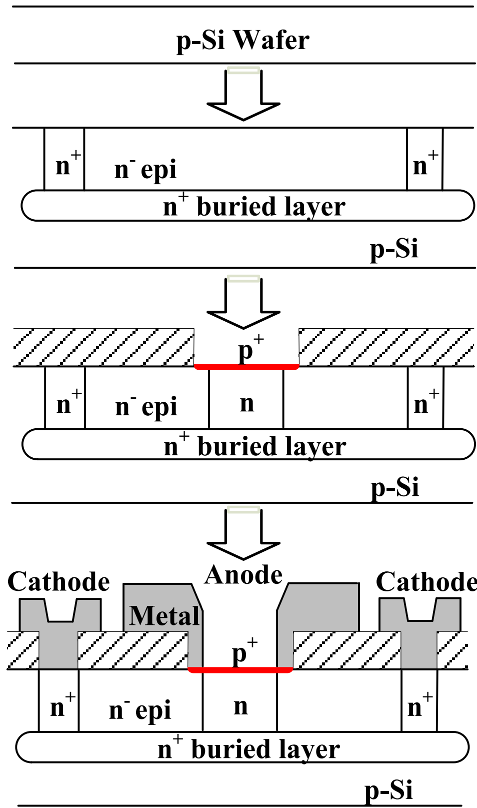

Fig. 1. Schematic process flow for the fabrication of a PureB SPAD.

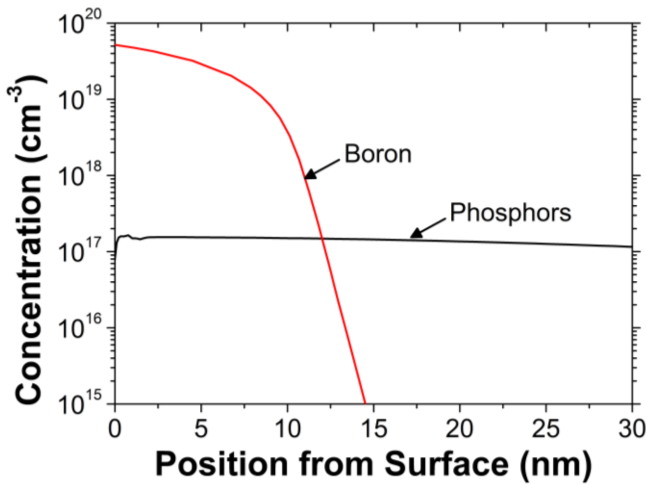

Fig. 2. Simulated doping profiles in the Si as a result of a 6-min PureB deposition at 700°C and drive in for 1 min at 850 °C on an n^- epi layer with doping 10^{15} cm^{-3}, and phosphorus implantations at 40 keV to a dose of 1×10^{12} cm^{-2} added to an implantation at 300 keV to a dose of 5×10^{12} cm^{-2}.

III. OPTICAL/ELECTRICAL CHARACTERIZATION

In Fig. 3 the current-voltage (I-V) characteristics are shown for a fabricated PureB SPAD with an anode of 4 µm in diameter and a light entrance window that is only 1 µm smaller in diameter. The diode ideality factor is almost 1 indicating that there are very few defects in the depletion region over the junction created by the PureB deposition. A very sharp and abrupt breakdown is observed and the V_{BD} is found to be around -14 V. The dark current before breakdown is below the detection limit and it increases to hundreds of microamperes past breakdown. A light emission test is shown in Fig. 4, which confirms that the onset of the breakdown is within the n-enrichment region and not at the anode edge.

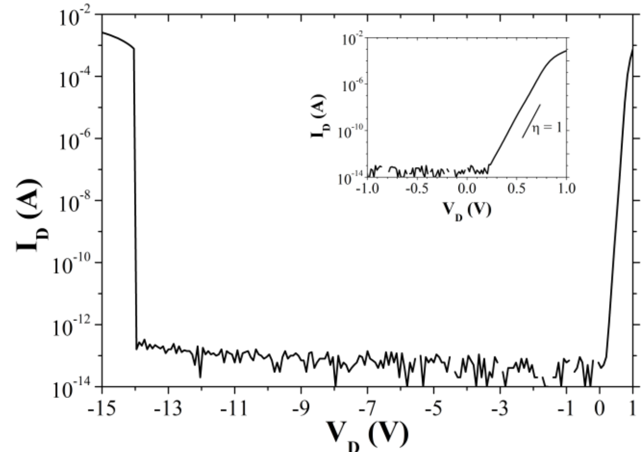

Fig. 3. I-V characteristics of aΦ4-µm PureB SPAD.

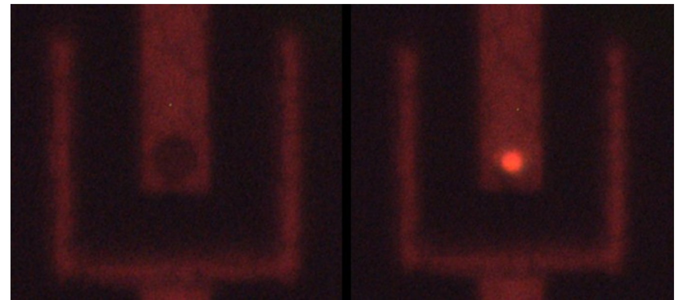

Fig.4. Light emission test for a PureB SPAD operating at a voltage of -14 V.

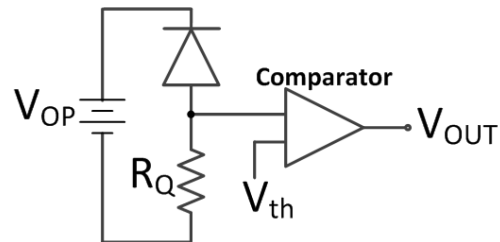

Fig. 5. Electronic schematic of a SAPD with passive quenching and passive recharge.

The basic circuit is shown in Fig. 5, for a SPAD operating in Geiger-mode with passive quenching and passive recharge via a ballast resistor R_Q, which is 100 kΩ in this case. The device is biased above breakdown (V_{BD}) by a voltage known

as the excess bias (V_{EB}), thus the operating voltage $|V_{OP}| = |V_{BD}| + V_{EB}$. At this high electrical field, an incoming photon can trigger an avalanche event. With the passive quenching mechanism, the high avalanche current must pass through R_Q, creating a voltage drop over the resistor that brings the voltage across the diode below breakdown. Thus the avalanching is stopped, the diode biasing is restored to the initial values, and a new incoming photon can be detected. This cycle takes an average time known as dead time. The avalanche pulses are sensed using a comparator with an appropriate threshold voltage V_{th}, thus converting the Geiger pulses into digital signals for photon counting.

Pulses can also be generated by non-photon-induced carriers, such as those originating from diffusion from the neutral regions, generation-recombination processes inside and near the multiplication region, band-to-band tunneling, or by the release of trapped carriers [5]. All these mechanisms result in dark counts, characterized by a parameter called dark count rate (DCR). As shown in Fig. 6, the DCR is measured at room temperature as a function of excess bias voltage V_{EB}. The DCR is extremely low, down to 5 Hz when V_{EB} = 0.5 V, presenting a low noise level at room temperature, which could be further reduced by cooling the device. In Fig. 7, a corresponding oscilloscope image taken with V_{EB} = 4.5 V displays a DCR of ~ 600 Hz.

The spectral sensitivity is evaluated by illuminating the device at different wavelengths with a light-source spot that is much larger than the diode area. The measured photocurrent I_D is compared with the photocurrent I_{REF} measured on a reference photodiode with an area larger than the spot size and for which the quantum efficiency is known for all wavelengths of interest. The ratio I_D/I_{REF} is plotted as a function of wavelength in Fig. 8 for the operating voltages of -10 V (below breakdown), -14 V (breakdown) and -20 V (Geiger-mode). The sensitivity shows a peak at 330 nm in Geiger-mode, where the optical gain is a 1000 times higher than that operating below breakdown and a 100 times higher than that operating right at the breakdown voltage.

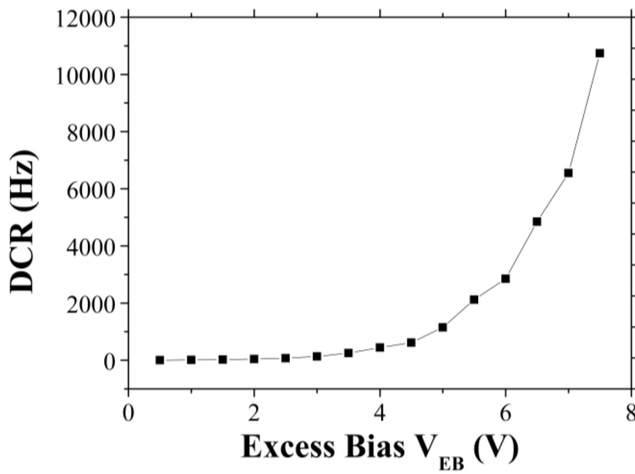

Fig. 6. DCR measurements of aΦ4-µm PureB Si photodiode as a function of excess bias voltage V_{EB} at room temperature.

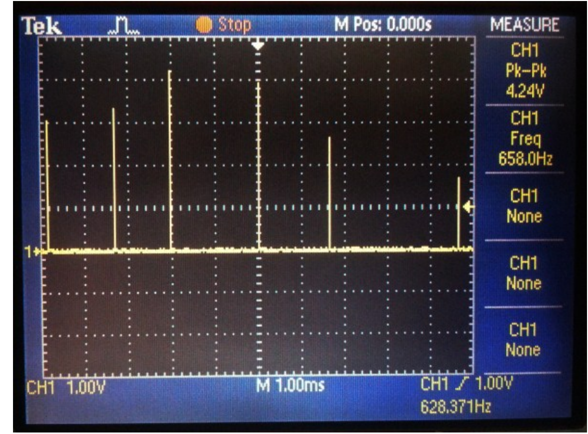

Fig. 7. Oscilloscope image of Geiger pulses in the absence of light at V_{EB} = 4.5 V. The sampling rate was sub-sampled in order to show more avalanche pulses.

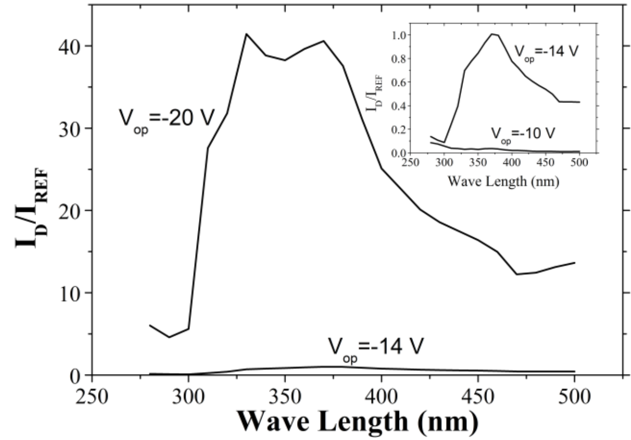

Fig. 8. I_D/I_{REF} of a Φ4-µm PureB SPAD in the UV spectrum for various operating voltages V_{OP}.

The Photon Detection Probability (PDP) is defined as the percentage of incoming photons that trigger an avalanche pulse at the incident light wavelength, which can be expressed as in equation (1):

$$PDP(\lambda) = \frac{A - DCR}{P} \quad (1)$$

In this equation, *A* is the avalanche pulse rate sensed by the SPAD in *Hz*; *P* is the incoming photon flux, given in *Hz* at wavelength λ, with which the active region of the SPAD is illuminated.

The PDP as a function of incident light wavelength is plotted in Fig. 9. The results display a good selectivity to the UV light, with a maximum PDP of around 10% at 370 nm. For this device, the peak of the PDP is in the UV spectrum, unlike the SPADs normally produced in CMOS technology, for which the peak is in the visible light spectrum [6]. This is in accordance with the fact that the p^+-n junction here only has a junction depth of ~ 12 nm and although the PureB layer itself is absorbing, it is only about 1 nm thick. For UV light the penetration depth in Si is less than 100 nm [7] and the

photon-generated carriers (electron – hole pairs) outside the depletion region can easily reach the multiplication region and cause an avalanche. However, for visible light, the penetration depth in Si increases with the wavelength and becomes hundreds of nm already at a wavelength of 500 nm. Then, the generated carriers will probably be swept into or be isolated in the substrate, thus recombining outside the multiplication region where no avalanche is triggered.

Moreover, due to the limitation of the measurement setup, the PDP measurement could only be performed down to 360 nm. Nevertheless, the PDP at shorter wavelength such as at 330 nm is expected to be significantly higher than 10 %.

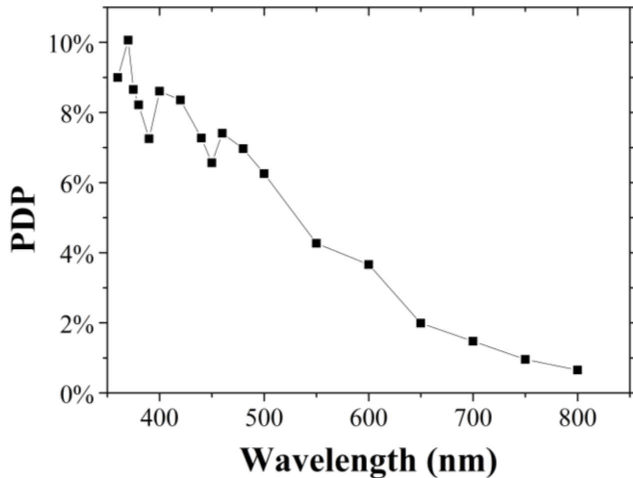

Fig. 9 Photon detection probabilityfor a Φ4-μm PureB SPAD as a function of wavelength with V_{EB} = 4.5 V.

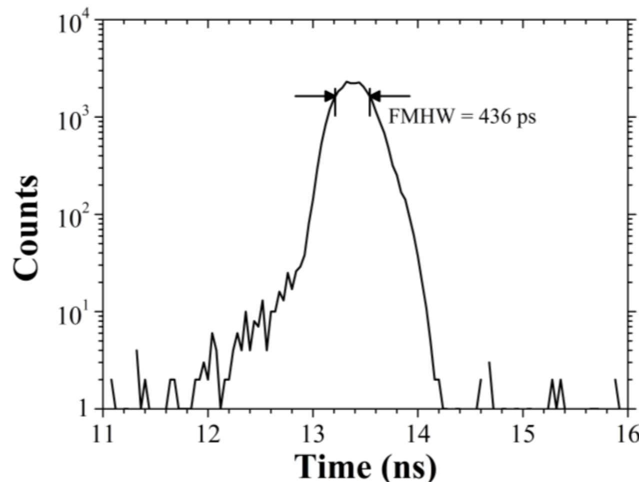

Fig. 10. Jitter performance of the Φ4-μm PureB SAPD when operated in Geiger Mode with V_{EB} = 4.5 V

The jitter performance is measured with the SPAD exposed to a 40 MHz pulsed laser source at a wavelength of 405 nm, and the light is attenuated to the single-photon level to prevent pile-up. The timing response is plotted in Fig. 10 for a Φ4-μm PureB SPAD with an excess bias voltage of 4.5 V. The measurement is obtained using the embedded time discriminator of a LeCroy WaveMaster 8600A. The measured Full Width at Half Maximum (FWHM) jitter is 436 ps.

IV. CONCLUSIONS

Highly UV-sensitive SPADs have successfully been fabricated by using PureB technology to create a nm-thin front-entrance window and a near-ideal p^+n junction diode. The use of an implanted n-enrichment layer in the central region of small circular anodes sets the breakdown voltage. When the diode is reverse biased, the leakage current is very low ($<10^{-12}$ A) below breakdown; this in turn is very abrupt (5 decades less than 100 mV) at -14 V. The device exhibits very low dark counts, with 5 Hz DCR at room temperature for a low excess bias of 0.5 V, and 10% PDP in the UV region at 370 nm. The absence of peripheral diffused p-type guard rings is beneficial for the fill factor. In this non-optimized version the diameter of the p^+-anode region is only 1 μm larger than the n-enrichment region, promising a high fill-factor for individual detectors and detector arrays.

ACKNOWLEDGMENT

The authors would like to thank the DIMES-ICP group for their help with processing and measurements. This work was financially supported by the Huygens Scholarship Programme of the Ministry of Education, Culture and Science (OCW) of the Netherlands.

REFERENCES

[1] L.K. Nanver, A. Sammak, V. Mohammadi, K. R. C. Mok, L. Qi, A. Šakić, N. Golshani, J. Derakhshandeh, T. M. L. Scholtes, W. D. de Boer, "Pure dopant deposition of B and Ga for ultrashallow junctions in Si-based devices", ECS Trans., vol. 49, nr. 1, pp. 25-33, 2012.

[2] L. Shi, S. Nihtianov, L. Haspeslagh, F. Scholze, A. Gottwald, L.K. Nanver, "Surface-Charge-Collection-Enhanced High-Sensitivity High-Stability Silicon Photodiodes for DUV and VUV Spectral Ranges," IEEE Transactions on Electron Devices, . Vol. 59, pp. 2888-2894, 2012.

[3] A. Šakić, V. Jovanović, P. Maleki, T. L.M. Scholtes, S. Milosavljević, L. K. Nanver, "Characterization of amorphous boron layers as diffusion barrier for pure aluminium," Proc. International Convention MIPRO 2010, Opatija, Croatia, pp. 52-55., 2010.

[4] E. Charbon, "Towards Large Scale CMOS Single-Photon Detector Arrays for Lab-on-Chip Applications", J. Phys. D: Applied Physics, Vol. 41, N. 9, May 2008

[5] R.H. Haitz, "Mechanisms Contributing to the Noise Pulse Rate of Avalanche Diodes," Journal of Applied Physics, Vol. 36, No. 10, October 1965.

[6] E. Charbon, M.W. Fishburn. "Monolithic Single-Photon Avalanche Diodes: SPADs," in Single-Photon Imaging. P. Seitz, A. Theuwissen , Ed. Heidelberg: Springer, Chapter 7, pp. 123-156.

[7] S. M. Sze and K. K. Ng, "Physics of Semiconductor Devices," Wiley India Pvt. Ltd., 2008 .